Elucidating the Transformation Pattern of the Cereal Allelochemical 6-Methoxy-2-benzoxazolinone (MBOA) and the Trideuteriomethoxy Analogue [D₃]-MBOA in Soil

THOMAS ETZERODT,[†,‡] SUSAN T. NIELSEN,[‡] ANNE G. MORTENSEN,[‡]
CARSTEN CHRISTOPHERSEN,[†] AND INGE S. FOMSGAARD*,[‡]

Chemical Institute, University of Copenhagen, Universitetsparken 5, DK-2100 Copenhagen, Denmark,
and Danish Institute of Agricultural Sciences, Research Centre Flakkebjerg,
DK-4200 Slagelse, Denmark

To deduce the structure of the large array of compounds arising from the transformation pathway of 6-methoxybenzoxazolin-2-one (MBOA), the combination of isotopic substitution and liquid chromatography analysis with mass spectrometry detection was used as a powerful tool. MBOA is formed in soil when the cereal allelochemical 2,4-dihydroxy-7-methoxy-1,4-benzoxazin-3-one (DIMBOA) is exuded from plant material to soil. Degradation experiments were performed in concentrations of 400 μg of benzoxazolinone/g of soil for MBOA and its isotopomer 6-trideuteriomethoxybenzoxazolin-2-one ([D₃]-MBOA). Previously identified metabolites 2-amino-7-methoxyphenoxazin-3-one (AMPO) and 2-acetylamino-7-methoxyphenoxazin-3-one (AAMPO) were detected. Furthermore, several novel compounds were detected and provisionally characterized. The environmental impact of these compounds and their long-range effects are yet to be discovered. This is imperative due to the enhanced interest in exploiting the allelopathic properties of cereals as a means of reducing the use of synthetic pesticides.

INTRODUCTION

Secondary metabolites from wheat, rye, and corn are known to have allelopathic activity. These metabolites, such as benzoxazolin-2-one (BOA) and 6-methoxybenzoxazolin-2-one (MBOA), have been investigated extensively for more than 15 years. An extensive list of the various acronyms and abbreviations used is given listed in **Table 1**. Major agricultural crops such as wheat (*Triticum aestivum*) and rye (*Secale cereale*) produce BOA and MBOA, respectively, from their corresponding hydroxamic acids 2,4-dihydroxy-1,4-(2*H*)-benzoxazin-3-one (DIBOA) and 2,4-dihydroxy-7-methoxy-1,4-(2*H*)-benzoxazin-3-one (DIMBOA). The hydroxamic acids are bound as glucosides in plant vacuoles and released by β-glucosidases upon disruption of cellular integrity (*1*). Further degradation products have been identified as 2-amino-3*H*-phenoxazin-3-one (APO) and 2-amino-7-methoxy-3*H*-phenoxazin-3-one (AMPO) from BOA and MBOA, respectively (*2–6*). The formation of the further degradation products is expected to occur through the action of several enzymes such as phenoxazine synthetase (*7–12*). The overall structure of the phenoxazine synthetase enzyme

has been determined by Kim et al. (*13*). The formation of APO from BOA was shown to occur through the intermediate 2-aminophenol. The formation of APO from 2-aminophenol occurred both as a chemical process and as a microbial process (*14*). Besides APO and AMPO, it has been shown that *N*-(2-hydroxyphenyl)malonamic acid (HPMA) and *N*-(2-hydroxy-4-methoxyphenyl)malonamic acid (HMPMA) have been identified in several cases from endophytic fungi (*1*, *15*, *16*). An understanding of the total process by which these allelopathic compounds are metabolized would give a better insight into the involved degradation products that might be formed and their environmental impact. Further possible metabolization of the AMPO derivatives by different enzymes in bacteria can be expected.

Many reversible enzymatic reactions are carried out by microorganisms including oxidation/reduction and acetylation/hydrolysis (*16*). AMPO itself is therefore a potential substrate.

The purpose of this study was to elucidate unknown degradation products from MBOA in soil using an isotope-labeled analogue of MBOA as well as to establish whether MBOA (and other methoxy-containing metabolites) undergoes demethylation followed by methylation.

The chemical structures of HPMA, HMPMA, DIBOA, and DIMBOA are given by Macias et al. (*17*). Structures other than these four are shown in **Table 2**.

* Corresponding author (telephone +45 89993610; fax +45 89993501; e-mail Inge.Fomsgaard@agrsci.dk).
† University of Copenhagen.
‡ Danish Institute of Agricultural Sciences.

1076 *J. Agric. Food Chem.,* Vol. 54, No. 4, 2006

Etzerodt et al.

Table 1. Acronyms and Abbreviations Used in This Paper

acronym or abbreviation	
^{13}C NMR	carbon nuclear magnetic resonance
^{1}H NMR	proton nuclear magnetic resonance
AAMPO	*N*-acetyl-2-amino-7-metoxy-3*H*-phenoxazin-3-one
abs EtOH	99% ethanol
AMPO	2-amino-7-metoxy-3*H*-phenoxazin-3-one
APO	2-amino-3*H*-phenoxazin-3-one
ASE	accelerated solvent extractor
BOA	benzoxazolin-2-one
bp	boiling point
[D$_3$]-	trideuterio-
DIBOA	2,4-dihydroxy-1,4(2*H*)-benzoxazin-3-one
DIMBOA	2,4-dihydroxy-7-methoxy-1,4(2*H*)-benzoxazin-3-one
ESI	electrospray ionization
EtOAc	ethyl acetate
GC-MS	gas chromatography interfaced to mass spectroscopy
HMNPAA	*N*-(2-hydroxy-4-methoxynitrophenyl)acetamide
HMNPHAA	*N*-(2-hydroxy-4-methoxynitrophenyl)-2-hydroxyacetamide
HMNPMA	*N*-(2-hydroxy-4-methoxynitrophenyl)malonamic acid
HMPAA	*N*-(2-hydroxy-4-methoxyphenyl)acetamide
HMPHAA	*N*-(2-hydroxy-4-methoxyphenyl)-2-hydroxyacetamide
HMPMA	*N*-(2-hydroxy-4-methoxyphenyl)malonamic acid
HPLC	high-performance liquid chromatography
HPMA	*N*-(2-hydroxyphenyl)malonamic acid
LC-MS	liquid chromatography interfaced to mass spectroscopy
m/z value	mass-to-charge ratio of ions formed in the mass spectrometer
MAP	2-amino-5-methoxyphenol
MBOA	6-methoxybenzoxazolin-2-one
MeCN	acetonitrile
MeOH	methanol
mp	melting point
RP18	reverse phase C18-column material
RT	retention time
TLC	thin-layer chromotography

MATERIALS AND METHODS

Chemicals. MBOA (98% purity, purchased from Lancaster Chemicals) and [D$_3$]-MBOA (95% purity) synthesized in our own laboratory were used for the degradation experiments. AMPO was provided by Dr. Scott Chilton, University of North Carolina, and Dr. Francisco A. Macías, University of Cadiz; AAMPO was provided by Dr. F. Macías. Characterization of AMPO and AAMPO and the determination of their purity were carried out by Dr. F. Macías (*17*). Purity was stated to be >98%.

The chemicals used for the synthesis of 6-trideuteriomethoxybenzoxazolin-2-one were the following: Propionic acid (99%) was purchased from Aldrich. Sodium hydride as a mineral oil suspension (60%) was purchased from Riedel-de-Haën. *p*-Toluenesulfonyl chloride (>97%), phenyl chloroformate (97%), and Pd on charcoal (5%) were purchased from Fluka Chemika. Metallic sodium (>99%), resorcinol (>99%), and sodium nitrite (99%) were purchased from Merck. Deuterated MeOH (99.8%) was purchased from Cambridge Isotopes. All solvents used were purchased from LAB SCAN as HPLC grades.

Analytical Equipment Used for Identification of Pure Compounds. GC-MS spectra were obtained on an HP GC5890-MS5972A Hewlett-Packard series II mass spectrometer. Direct inlet mass spectra were obtained on a JEOL JMS-HX110A tandem mass spectrometer. ^{1}H NMR spectra were recorded on a Varian 300 MHz instrument. ^{13}C NMR and correlated spectra (COSY, HETCOR) were recorded on a Unity 400 MHz spectrometer. Infrared spectra were recorded as a KBr sandwich using a Perkin-Elmer FT-IR spectrometer 1760X. Elementary analyses were performed with a Flash EA 1112 series, CE instrument.

Synthesis of 6-Trideuteriomethoxybenzoxazolin-2-one. *Trideuteriomethyl p-Toluenesulfonate (1).* The compound was prepared following essentially the directions given by Quast and Bieber (*18*). Sodium hydride (30 g, 60%, 0.78 mol) was placed in a dry round-bottom flask (500 mL). Diethyl ether (100 mL) was added, the suspension was magnetically stirred, the hydride was allowed to settle for 10 min, and the ether was decanted. Because NaH has a density of
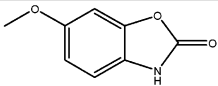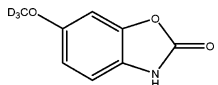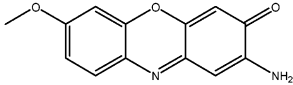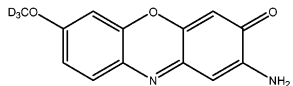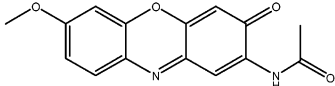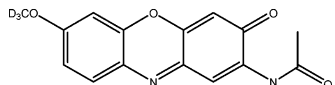
0.92 g/mL and diethyl ether a density of 0.71 g/mL, this procedure when repeated four times left ~90% of the NaH essentially free of mineral oil. After the last washing, dry THF (150 mL) and *p*-toluenesulfonyl chloride (49.7 g, 0.26 mol) were added, the stirring was started, and the mixture was cooled to −5 °C. While the temperature was held below 0 °C, trideuteriomethanol (10 g, 0.28 mol) was added dropwise during 1 h. The reaction mixture was stirred further for 4 days at room temperature, and diethyl ether (130 mL) added. Water (90 mL) was added dropwise, at first followed by a vigorous evolution of hydrogen due to unreacted sodium hydride. An additional amount of water was added until all precipitate had dissolved, and the aqueous phase was separated and washed three times with ethyl ether (100 mL). The combined organic phases were dried with magnesium sulfate, the solvent was removed in vacuo, and the residue was distilled (bp 117 °C/2.5 mbar) to give colorless **1** (23.58 g, 48% yield): GC-MS, *m/z* 189 (M$^{•+}$, 48), 155 (40), 107 (15), 91 (100), 65 (38); ^{1}H NMR (CDCl$_3$), δ 7.71 (d, 2H, H$_A$, *J* = 8.2 Hz), 7.29 (d, 2H, H$_B$, *J* = 8.2 Hz), 2.38 (s, 3H, CH$_3$); ^{13}C NMR (CDCl$_3$), δ 144.7 (C4), 132.1 (C1), 129.7 (C3), 127.9 (C2), 21.5 (CH$_3$); IR (cm^{-1}) 3067 w (CH), 2926 mw (CH), 2263 w−2087 w (CD), 1598 m, 1494 m and 1451 m (arom C=C), 1363 s and 1180 s (S=O), 1104 s (C−O), 996 s, 817 s, 741 s (S−O−C). Found: C, 50.72; S, 16.99. Calcd for C$_8$H$_7$D$_3$O$_3$S: C, 50.77; H, 6.92; S, 16.94.

Resorcinol-O-mono-trideuteriomethyl Ether (2). Synthesis of **2** was carried out following the directions given by Bird et al. (*19*). With magnetic stirring, sodium metal (5.72 g, 0.249 mol) was dissolved in MeOH (240 mL, dried over molecular sieves), maintaining gentle reflux. Resorcinol (52.9 g, 0.48 mol) was added in one portion. The solution first turned dark orange and then light yellow, indicating changes in equilibrium. Addition of **1** (22.72 g, 0.12 mol) followed by further reflux for 2.5 h was followed by changes in color from violet/black to orange/yellow. Water (70 mL) was added, followed by 4 M NaOH until a pH of 11 was reached, where both the mono-[D$_3$]-methyl ether and resorcinol were converted to salts. The dimethyl ether was removed by extraction three times with 100 mL of toluene and discarded. Acidification to pH 1 with 3 M HCl liberated the phenols. The monomethyl ether **2** was secured by extraction with toluene (100 mL, 9 times) (*20*), in which resorcinol is almost insoluble. The combined toluene phases were dried with MgSO$_4$ and evaporated in vacuo, yielding 9.4 g, 62%, of crude product. Both NMR and GC-MS indicated that resorcinol was present in the product in a 1−5% amount. The crude product was used without further purification for the synthesis of compound **3**: MS (DI), *m/z* 127 (M$^{•+}$, 85), 110 (100), 95 (30), 81 (34); ^{1}H NMR (CDCl$_3$), δ 7.14 (t, 1H, H-5), 6.50 and 6.44 (dd, each 1H, *J* = 7 and 2 Hz, H-4 and H-6), 6.42 (s, 1H, H-2), 4.57 (brs, 1H, OH); ^{13}C NMR (CDCl$_3$), δ 101.4, 106.3, 107.7, 130.0, 156.5, 160.8; IR (cm^{-1}) 3387 s, br (OH), 2221 m and 2073 m (CD), 1597 s and 1490 s (arom C=C), 1293 s and 1153 s (C−O), 1017 ms, 960 m, 898 m, 838 ms, 765 ms, 685 ms.

The synthesis of **3** and **4** was carried out following the directions given by Maleski (*21*).

2-Nitro-5-trideuteriomethoxyphenol (3). Crude **2** (7.63 g, 60 mmol) was dissolved in propionic acid (60 mL). The solution was cooled to approximately −5 °C, and during the following operations the temperature was kept below 0 °C to minimize polynitration. With stirring, another solution of NaNO$_2$ (4.2 g, 60.9 mmol) in water (10 mL) was added dropwise, giving a deep red mixture. The resulting slurry was stirred for a further 1 h, and HNO$_3$ (100%, 7.58 g, 120.3 mmol) was added dropwise under a nitrogen atmosphere. The slurry was stirred for 1 h and allowed to warm to room temperature (2 h). Water (50 mL) was added slowly, the precipitate was filtered by suction, and finally washing with 50% of aqueous propionic acid (60 mL) left a curry-yellow product. Drying over KOH in vacuo yielded pure **3** (3.33 g, yield 32%): mp 91−92 °C; MS (DI), *m/z* 172 (M$^{•+}$, 100), 156 (3), 142 (54), 114 (71); ^{1}H NMR (DMSO-d_6), δ 7.96 (d, 1H, *J* = 9.1 Hz, H-5), 6.62 (d, 1H, *J* = 2.6 Hz, H-2), 6.58 (dd, 1H, *J* = 2.6, 9.1 Hz, H-4); ^{13}C NMR (CDCl$_3$), δ 157.97, 127.0, 109.5, 101.4; IR (cm^{-1}) 3195 w (OH), 2242 w, 2199 w and 2078 w (CD), 1620 s, 1591 s and 1527 m (*m*) (arom C=C), 1489 m and 1324 m (N=O), 1283 (C−O), 1204 m, 1094 s, 977 m, 834 m, 757 m, 676 m, 628 m. Found: C, 48.97; N, 8.08. Calcd for C$_7$H$_4$D$_3$NO$_4$: C, 48.84; H, 5.85; N, 8.14.

Fate and Effects of Allelochemicals

J. Agric. Food Chem., Vol. 54, No. 4, 2006 **1077**

Table 2. MBOA, [D₃]-MBOA, and Their Metabolites and Parameters for the Various Compounds Discussed in This Paper

compound	acronym	mass	molecular structure	retention time (min.)	mode of measurement
6-methoxy-benzoxazolin-2-one	MBOA	165		14.7	ESI+
6-trideuterio-methoxy-benzoxazolin-2-one	D3-MBOA	168		14.7	ESI+
2-amino-7-methoxy-phenoxazin-3-one	AMPO	242		17.5	ESI+
2-amino-7-trideuterio-methoxy-phenoxazin-3-one	D3-AMPO	245		17.5	ESI+
2-acetyl-amino-7-methoxy-phenoxazin-3-one	AAMPO	284		18.2	ESI+
2-acetyl-amino-7-trideuterio-methoxy-phenoxazin-3-one	D3-AAMPO	287		18.2	ESI+

6-[D₃]-Methoxy-2(3H)-benzoxazolone (4). Water (∼5 mL) was transferred into a 250-mL round-bottom flask. Formic acid (1.72 mL, 0.044 mol) was added, followed by KOH (2.51 g, 0.045 mol) dissolved in abs EtOH (25 mL). Magnetic stirring and a N₂ atmosphere were applied during the whole procedure. Pd on charcoal (5%, 0.0574 g) was transferred to the reaction mixture along with **3** (2.25 g, 0.013 mol). The resulting slurry was heated for 3 h at 70 °C while the color changed from green to black. The reaction was completed after 2.5 h as indicated by TLC (40% EtOAc in *n*-heptane, alumina plates coated with silica gel 60 F₂₅₄ obtained from Merck). After the contents of the flask had cooled to room temperature, degassed water (7.5 mL) was added. Phenyl chloroformate (PCF, 2.324 g, 0.014 mol) was transferred via syringe and cannula to the reaction mixture, keeping the temperature at 25−30 °C during the addition. The mixture was cooled to 25 °C, and the resulting cherry red slurry was stirred for a further 0.5 h. A solution of NaOH (0.5934 g, 0.015 mol) in degassed water (11 mL) was added, followed by heating until a temperature of 45−50 °C was reached. The mixture was allowed to react for 1 h at this temperature, filtered, and washed with 50% of EtOH. Aqueous HCl (10%) was added to the combined filtrates, resulting in precipitation of product **4**.

The crude product was separated using a glass column equipped with RP18 (15 μm) material (*h*, 3.8 cm; ∅, 2.2 cm) (obtained from Novo Nordisk A/S). A gradient of MeCN in water was used, starting with 30% of MeCN and increasing by 5% of MeCN until the first fraction of [D₃]-MBOA was observed. The chromotographing was then continued isocratically. Recrystallization from toluene yielded pure light reddish **4** (223.1 mg, yield 55%): mp 151.5−153 °C; MS (DI), *m/z* 168 (M•⁺, 100), 150 (35), 139 (5), 122 (8), 112 (10), 106 (18); ¹H NMR (CDCl₃), δ 8.42 (br s, 1H, NH), 6.95 (d, 1H, *J* = 8.8 Hz, H-4), 6.83 (d, 1H, *J* = 2.3 Hz, H-7), 6.71 (dd, 1H, *J* = 8.8 Hz, 2.34 Hz, H-5); ¹³C NMR (CDCl₃), δ 156.1 (C3), 155.9 (C=O), 144.5 (C1), 122.5 (C6), 110.0 (C5), 109.6 (C4), 97.5 (C2), 29.6 (CD₃); IR (cm⁻¹) 3166 s (NH), 3113 s and 3020 m (CH), 2260 w and 2074 w (CD), 1785 vs (C=O), 1635 mw and 1460 mw (arom C=C), 1496 vs (NH), 1319 s (C−N), 1208 ms−1097ms (C−O), 881 w, 845 m. Found: C, 56.88; N, 8.15. Calcd for C₈H₄D₃NO₃: C, 57.14; H, 5.99; N, 8.33.

Experimental Design of Degradation Studies. Two series of degradation experiments for the benzoxazolinone compounds were performed at 400 μg/g of soil. The experiments were performed with MBOA and with the trideuterated analogue 6-deuteriomethoxybenzoxazolin-2-one ([D₃]-MBOA). A blank soil incubation series was included as well, sampling and analyzing at the same time intervals as the benzoxazolinone incubations. The same soil was used for all of the experiments. A total of 59 soil samples, including control, stability, MBOA and [D₃]-MBOA samples, were incubated in the dark at 17 °C. At preselected time intervals (see Samples) the incubation of selected samples was interrupted and the samples were freeze-dried and extracted for analysis.

Soil Data. Sandy loam soil (Typic Agrudalf, classified according to USDA Soil Taxonomy) (*22*) was collected in September 2003 from the upper 0−10 cm at Nørregård, a cultivated field near the Research Center Flakkebjerg, Denmark. The field had previously been cultivated with spring-sown barley in 2001, 2002, and 2003. The upper 0−10 cm of soil was passed through a fine 2.0-mm sieve to separate larger objects such as stones and plant parts, leaving only finer particles of soil. It was stored at −17 °C until experimental usage. The characteristics of the soil were as follows: fine sand (0.063−0.2 mm), 31.2%; coarse sand (0.2−2.0 mm), 24.2%; silt (2−20 μm), 15.0%; coarse silt (20−63 μm), 8.8%; clay (<2 μm), 18.0%; humus, 2.8%; potassium, 5.9%; phosphorus, 1.7%; magnesium, 6.2%; pH 6.8.

Degradation Experiment. Five grams of chemically and microbially inert Ottawa sand (particle size, 20−30 mesh; Fisher Chemicals) was added to a 100 mL Erlenmeyer flask. Methanolic solutions of MBOA or [D₃]-MBOA were added to obtain a final concentration of 400 μg/g of soil for each incubation sample. Addition of the compounds in methanolic solution to Ottawa sand and subsequent evaporation of methanol was used to improve the distribution of MBOA and [D₃]-MBOA in soil added as follows: 11.48 g of moist Nørregård soil corresponding to 10 g of dry soil was added to the 100 mL flask and mixed; 0.52 mL of water was added to obtain a water content corresponding to a measured field capacity of 17.4% water content.

The flask was closed with a rubber stopper with cotton allowing air circulation. All samples were incubated in the dark at 17 °C.

Samples. Incubations were terminated after 0, 2, 4, 7, 9, 14, 18, 22, 26, 33, 46, 60, 75, 90, and 105 days for control, MBOA, and [D₃]-MBOA. Each sample was stored at −17 °C until freeze-drying followed by extraction by accelerated solvent extraction (ASE). Before ASE, the freeze-dried samples were crushed homogeneously.

Extraction. The extraction was performed on an accelerated solvent extractor (from Dionex) for each sample. The freeze-dried samples were transferred to an extraction cell (30 mL) followed by extraction with acidified methanolic solution (0.5%). The program for the extraction procedure was as follows: preheat, 5 min; heat, 50 min; static, 5 min; flush, 60%; purge, 60 s; cycles, 2; pressure, 1500 psi; temperature, 80 °C. Subsequently the samples were evaporated to a volume of 20 mL with a N₂ flush in a TurboVap LV evaporator from Zymark. Finally, all extracts were stored at −17 °C until analysis by LC-MS.

Analysis. The samples were analyzed with LC-MS on a Sciex API 2000 model from Applied Biosystems. ESI was used as ionization method, obtaining spectra in both positive and negative modes according to the difference in sensitivity of the analytes for the two modes. For the chromatographic part a RP18 BDS Hypersil column, 250 × 2.1 mm, particle size = 5 μm and pore size = 130 Å, was used. Two mobile phases (A, 10% MeOH in water; and B, MeOH, both containing 20 μM glacial acetic acid) were used in a gradient system as follows with a flow rate of 200 μL/min: step 0, 0−1 min, 90% A + 10% B; step 1, 1−8 min, 30% A + 70% B; step 2, 8−15 min, 30% A + 70% B; step 3, 15−16 min, 90% A + 10% B; step 4, 16−23 min, 90% A + 10% B. Standard solutions of MBOA, AMPO, and AAMPO were prepared in methanol and used for verification of the signals of these compounds. Recovery experiments for validation of the extraction method have been performed earlier. The recoveries were 89% for MBOA, 35% for AMPO, and 65% for AAMPO (*23*).

RESULTS AND DISCUSSION

Several types of microorganisms are responsible for the enzymatic transformation of secondary metabolites. This transformation includes hydroxylation by hydroxylases such as regio- and chemoselective *non-heme* iron-monoxidases (*24−28*), regioselective *flavoprotein monoxygenases* (*28−30*), and *cytochrome P450 enzymes* (*31*). The latter is neither regio- nor chemoselective, giving rise to several possible hydroxylated derivatives. Furthermore, N-oxidation is possible by *flavoproteins* and *cytochrome P450 enzymes* (*32−36*). Additional metabolization is also possible via *methyl transferases* (upon previous introduction of OH groups) (*37*) and *N-acetyl transferases*.

Fomsgaard et al. (*38*) published a review on microbial transformation products of BOA, MBOA, and 2-hydroxy-1,4-benzoxazin-3-one (HBOA). The compounds that were listed in the review, formed from BOA, MBOA, or HBOA by fungi in liquid media, were N-(2-hydroxyphenyl)acetamide and further hydroxy- and nitro-substituted derivatives thereof, N-(2-hydroxyphenyl) malonamic acid, N-(2-hydroxy-4-methoxyphenyl)malonamic acid, APO, various hydroxylated and acetylated substitutes of APO, and AMPO (*1*, *15*, *16*, *39*, *40*). APO, AMPO, and in some cases the acetylated derivative have been reported as soil transformation products of BOA and MBOA (*2−6*, *14*, *23*). A 4-acetyl derivative of BOA has also been observed (*41*).

Several *m/z* values corresponding to the different possible hydroxy and methoxy derivatives of the APO structure were investigated. A large number of metabolites from BOA and MBOA are supposed to be identical or analogously formed. Thus, a reasonable hypothesis regarding *m/z* values to search for could be established.

For an overview of the parent APO structure with possible positions for oxidation, see **Figure 1**. Metabolites identified in previous studies and methoxylated analogues are shown in
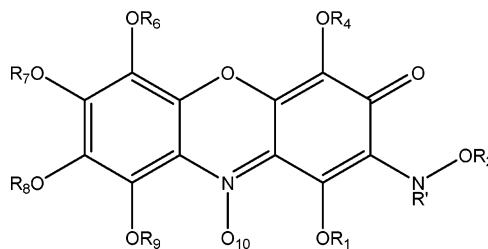

Figure 1. Aminophenoxazine basic structure with possible sites for oxidation indicated by R1–R9 and O10. R′ = H, Ac.

Table 2. Novel theoretical metabolites yet to be verified are presented in **Table 3**.

We verified new masses using both MBOA and its trideuterated analogue 6-trideuteriomethoxybenzoxazolin-2-one to establish whether unknown transformation products still contained the 6-methyl group or not. By using LC-MS we could control this by investigating an array of *m/z* values from ESI⁺ and ESI⁻ mass spectrometry. Compounds exhibiting the same transformation pattern as well as the same retention time (RT) for the same *m/z* value for both transformation series (MBOA and D3-MBOA) no longer contained the methyl group from the original 6-position in MBOA and [D₃]-MBOA. If the *m/z* values differed by 3 according to the mass difference of the MeO and D₃CO groups, all other factors being equal the transformation products still contained the original methyl group. The detection of *m/z* values higher than the corresponding mass of MBOA and [D₃]-MBOA appearing at the same RT as MBOA and [D₃]-MBOA and with uniform transformation patterns was caused by the formation of adducts of MBOA and [D₃]-MBOA, respectively. This was controlled using external standards for MBOA and [D₃]-MBOA. The results of all samples were compared with results from blank soil, incubated for the same time interval and analyzed with the same procedure. The measurements from the blank samples were subtracted from the measurements of the benzoxazolinone samples.
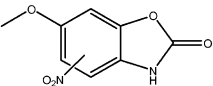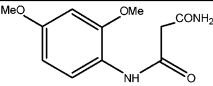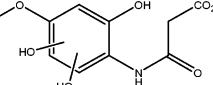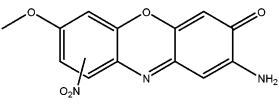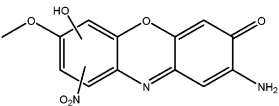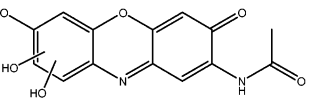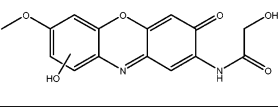
For transformation products discovered in this experiment, consult **Schemes 1** and **2**, respectively. In the schemes are also given the possible relationship between the respective metabolites.

The experiments were initiated by adding MBOA and [D₃]-MBOA to soil in order to identify the outcoming transformation products. Therefore, the transformation patterns for these compounds were determined initially. For ESI⁺ [MBOA + H]⁺, *m/z* 166, and for [[D₃]-MBOA + H]⁺, *m/z* 169 (RT = 14.7 min) the observed transformation was plotted as the area of the signals as a function of time (see **Figure 2**). This unique transformation pattern was repeatedly observed for several adduct ions besides the [MBOA + H]⁺ ion, including the Na⁺ adduct. It was notable that the transformation was very rapid. The same unique pattern was observable in ESI⁻ ([MBOA − H]⁻, *m/z* 164) for which only the course of MBOA is plotted (**Figure 3**) as it is representative of both compounds according to the ESI⁺ mode.

Verification of *m/z* 243 (for MBOA incubation samples) and 246 (for [D₃]-MBOA incubation samples) in ESI⁺ was certainly observed as signals appeared at the same RT (17.5 min) illustrated in **Figure 4**. These *m/z* values correspond to [AMPO + H]⁺ and [[D₃]-AMPO + H]⁺.

In studies by Gents et al. (*2*) a chromatographic method very similar to ours was used. In that study BOA appeared at RT = 14.0 min, APO at RT = 17.0 min, and AAPO at RT = 17.5 min. In the present studies MBOA appeared at 14.7 min, and by analogy with this AMPO/[D₃]-AMPO should appear at ∼17.7

Fate and Effects of Allelochemicals

J. Agric. Food Chem., Vol. 54, No. 4, 2006   **1079**

Table 3. Parameters for the Various Possible Compounds Discussed in This Paper According to Our Hypotheses[a]

compound	mass	molecular structure	retention time (min.)	mode of measurement
nitro-MBOA	210 / 213		13.9	ESI-
N-(2,4-dimethoxy-phenyl)-malonamic amide	240 / 246		20.5	ESI+
dihydroxy-HMPMA	257 / 260		17.2	ESI+
nitro-AMPO	287 / 290	isomer of	17.3	ESI+
hydroxy-nitro-AMPO	303 / 306	isomer of	16.1	ESI+
N-(acetyl)-dihydroxy-AMPO or N-(hydroxyacetyl)-hydroxy-AMPO	316 / 319	isomer of or	16.5	ESI-

[a] For all isomers N-oxidation is included as an isomeric compound as well. For each compound two masses are shown: the first for the nonlabeled compound and the second for the labeled compound.

min and AMPO/[D$_3$]-AAMPO at ~18.2 min (for these acetylated derivatives, see below).

This was consistent with the observed RT for these *m/z* values, which were determined to be AMPO and [D$_3$]-AMPO. The identity of AMPO was confirmed by comparison with the retention time and mass spectra of a pure AMPO standard.

Both AMPO and its isotopomer were present in only small amounts on day 0, ascending to constant significant levels from day 20 through day 105 (see **Figure 4**). If further transformation products should be formed, the velocity of transformation of AMPO/[D$_3$]-AMPO must be almost equal to the velocity of formation because no net change in area and thereby concentration is observed.

In contrast to earlier studies of transformation of MBOA (*4*) the concentration of formed AMPO remained constant, whereas Kumar et al. (*4*) showed that the concentration of AMPO decreased after day 20. The transformation rate is concentration dependent (*6*). In the studies by Understrup et al. (*3*) APO formed from BOA reached a maximum concentration at day 7 and was completely transformed after 20 days at a concentration of 0.4 mg of BOA added/g of soil, whereas at 4 mg of BOA

added/g of soil APO reached the maximum concentration at day 50, after which a decrease in concentration of APO was observed.

Studies concerning MBOA and its transformation into AMPO at a concentration of 0.4 mg of MBOA added/g of soil (*6*) showed AMPO to have only a slight decrease in concentration after day 20. That was the same concentration of MBOA as studied in this paper. In this paper levels of AMPO appeared to be constant. The difference could be due to the fact that different kinds of soil were used. This might cause a difference in the pattern of formation and disappearance of AMPO due to possible differences in the microbial environment in different kinds of soil.

Fomsgaard et al. (*6*) showed that AAMPO was formed from AMPO by microorganisms in soil. This could be confirmed by the results presented in this paper. **Figure 5** shows the time-dependent course of formation of AAMPO and [D$_3$]-AAMPO.

In ESI$^+$ with RT of 18.2 min *m/z* 285 and 288 corresponding to [AAMPO + H]$^+$ and [[D$_3$]-AAMPO + H]$^+$ were observed with a transformation pattern similar to that observed for AMPO and [D$_3$]-AMPO. Only the levels at which the signals were

1080 *J. Agric. Food Chem.,* Vol. 54, No. 4, 2006

Etzerodt et al.

Scheme 1. Metabolites Formed from MBOA in Biotransformation by Microorganisms in Soil[a]
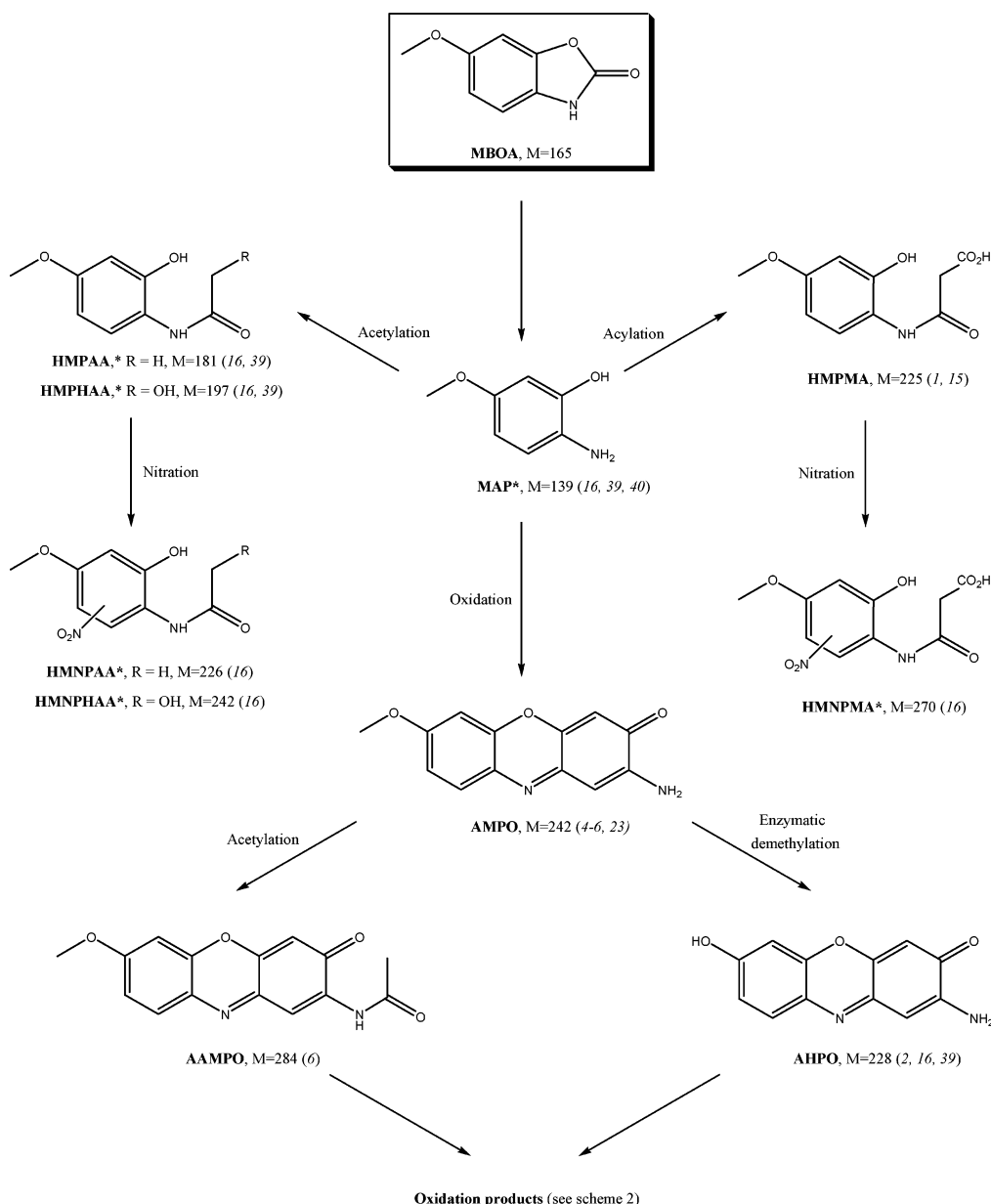
[a] Degradation products are illustrated along with their acronyms and mass values.

detected relative to AMPO were significantly smaller as also shown by Kumar et al. (*4*) and Fomsgaard et al. (*6*).

As stated previously, a comparison with Gents et al. (*2*) was possible regarding RT, and certainly a RT of 18.2 min was observed, confirming the identity of these *m/z* values. The identity of AAMPO was additionally confirmed by comparison of retention time and mass spectrum with the retention time and mass spectrum of a pure standard of AAMPO dissolved in methanol and injected into the chromatographic system.

Figures 4 and **5** show that AMPO and [D$_3$]-AMPO are formed first, followed by the acetylation to AAMPO and [D$_3$]-AAMPO.

For measurements using ESI$^-$, *m/z* 209 and 212 corresponding to masses 210 and 213, respectively, were observed at RT = 13.9 min. The signal appeared with a maximum at day 0 and decreased rapidly until day 10, when it reached a minimum, which remained constant as shown in **Figure 6**. It was observed for both the MBOA and the [D$_3$]-MBOA incubation samples.

The transformation product (masses 210 and 213) has provisionally been characterized to be nitro-MBOA.

Because this metabolite appeared in the [D$_3$]-MBOA incubation samples 3 *m/z* values higher relative to the MBOA incubation samples, the integrity of the trideuteriomethoxy group was conserved. The formation of this metabolite from MBOA and [D$_3$]-MBOA was very rapid, because the maximum signal of the metabolite was observed at day 0. In ESI$^+$ *m/z* 241 and 247 could be correlated, having the same RT = 20.5 min (**Figure 7**), the first for the MBOA samples and the latter for the [D$_3$]-MBOA samples corresponding to masses 240 and 246, respectively. The signals were detected with a similar area. The patterns of these curves were comparable to those for AMPO and [D$_3$]-AMPO. Both kinds of metabolites were formed to a maximum around day 20, after which a constant level was seen.

This was believed to be *N*-(2,4-dimethoxyphenyl)malonamic amide. The existence of methyl-accepting chemotaxis proteins (MCPs) (*42*) indicated the possibility of transformation products

Scheme 2. Possible Structure of Metabolites Provisionally Identified from MBOA in Biotransformation by Microorganisms in Soil[a]
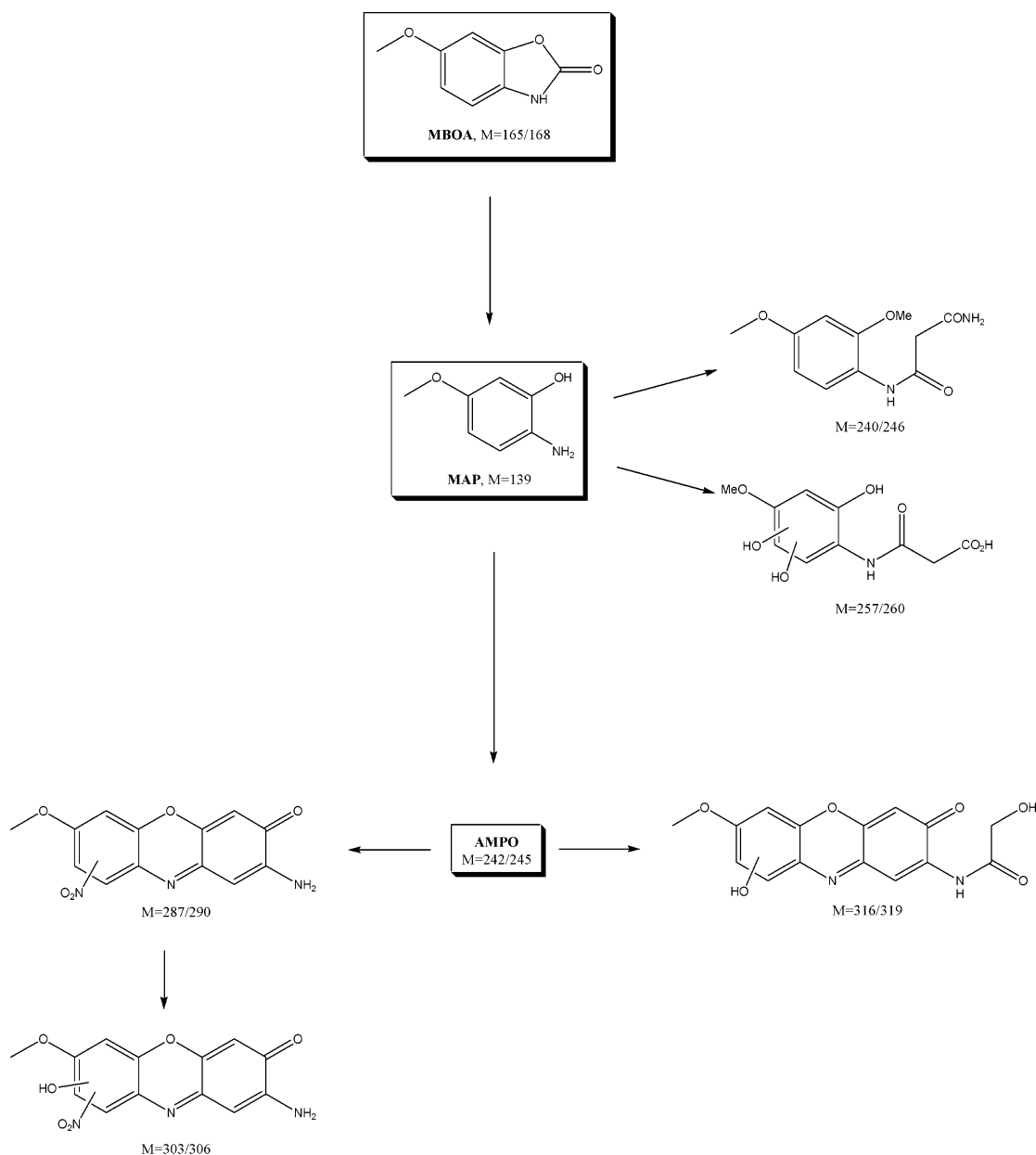
[a] Degradation products are illustrated along with their acronyms and mass values.

from MBOA being methylated. The enzymes involved in the studies by Albert et al. (*42*) used *S*-adenosylmethionine as the methyl-transferring agent. For a certain amount of substrate

present, equilibrium between different degrees of methylation occurs. Therefore, it is plausible to assume the same to be
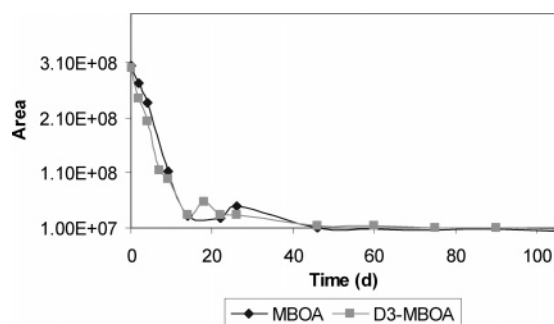

Figure 2. Transformation of MBOA (*m/z* 166) and [D$_3$]-MBOA (*m/z* 169) measured using ESI+ (RT = 14.7 min). Area is measured as a function of time. Degradation experiment was performed in Flakkebjerg soil with initial concentrations of 400 μg/g of MBOA and [D$_3$]-MBOA.
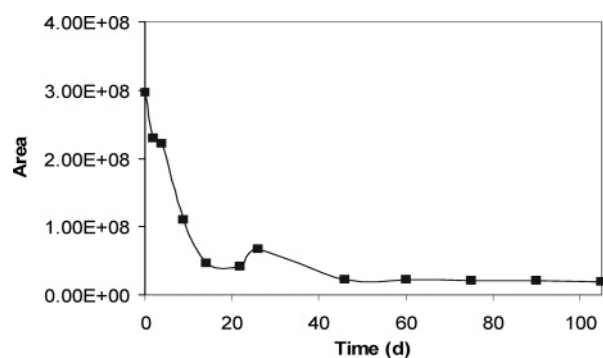

Figure 3. Transformation of MBOA (*m/z* 164) measured using ESI− (RT = 14.7 min). Area is measured as a function of time. Degradation experiment was performed in Flakkebjerg soil with an initial concentration of 400 μg/g of MBOA.
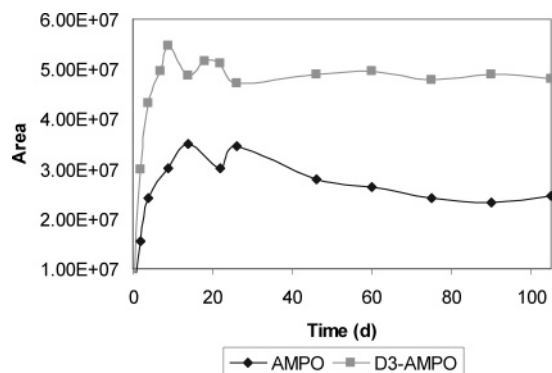
Figure 4. Formation and disappearance of AMPO (*m/z* 213) and [D$_3$]-AMPO (*m/z* 216) from MBOA and [D$_3$]-MBOA, respectively, measured using ESI$^+$ (RT = 17.5 min). Area is measured as a function of time. Degradation experiment was performed in Flakkebjerg soil with initial concentrations of 400 μg/g of MBOA and [D$_3$]-MBOA.

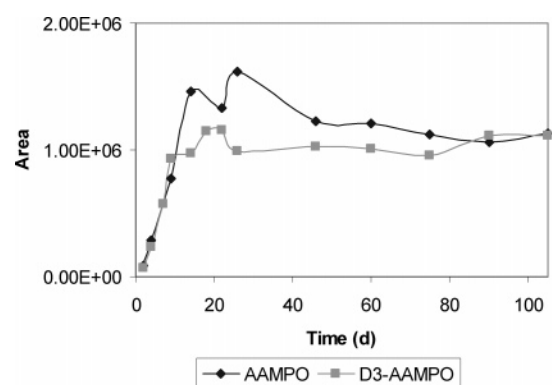**Figure 5.** Formation and disappearance of AAMPO (*m/z* 255) and [D$_3$]-AAMPO (*m/z* 258) measured using ESI$^+$ (RT = 18.2 min). Measured area is a function of time. Degradation experiment was performed in Flakkebjerg soil with initial concentrations of 400 μg/g of MBOA and [D$_3$]-MBOA.

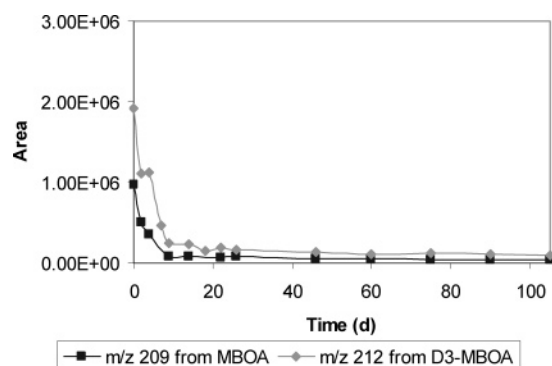**Figure 6.** Formation and disappearance of mass 210 (*m/z* 209) and 213 (*m/z* 212) from MBOA and [D$_3$]-MBOA, respectively, measured using ESI$^-$ (RT = 13.9 min). Area is measured as a function of time with initial concentrations of MBOA and [D$_3$]-MBOA of 400 μg/g in Flakkebjerg soil.

possible for the microorganisms in soil responsible for the transformation of MBOA and its degradation products.

Because the difference in mass between the transformation product from the nonlabeled and the labeled MBOA was 6, two of the original methyl groups appeared to be present. This was most likely due to the formation of a methylating pool. This pool could convert an appropriate methoxyphenol to the corresponding dimethoxy derivative by methylation of the phenolic OH group. Yue et al. (*1*) showed that aminophenols are transformed into malonamic acids by microorganisms such
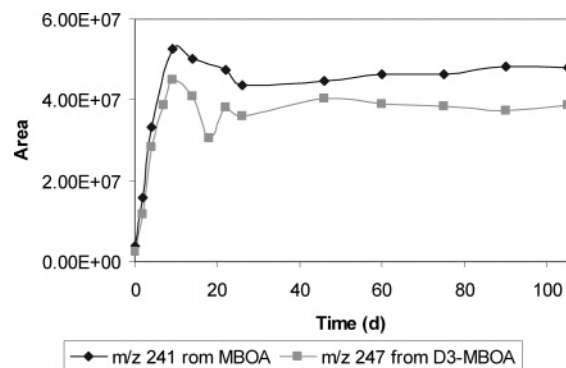

Figure 7. Formation and disappearance of mass 240 (*m/z* 241) and 246 (*m/z* 247) from MBOA and [D$_3$]-MBOA, respectively, measured using ESI$^+$ (RT = 20.5 min). Area is measured as a function of time with initial concentrations of MBOA and [D$_3$]-MBOA of 400 μg/g in Flakkebjerg soil.

Figure 8. Formation and disappearance of mass 257 (*m/z* 258) and 260 (*m/z* 261) from MBOA and [D$_3$]-MBOA, respectively, measured using ESI$^+$ (RT = 17.2 min). Area is measured as a function of time with initial concentrations of MBOA and [D$_3$]-MBOA of 400 μg/g in Flakkebjerg soil.
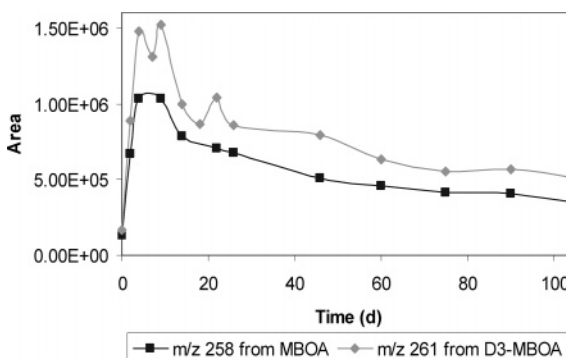
as fungi, which also supports the theory that this compound could be *N*-(2,4-dimethoxyphenyl)malonamic amide. See **Table 3** for the structural formula. For the MBOA and [D$_3$]-MBOA incubation samples, masses 257 and 260 were observed as *m/z* 258 and 261, respectively, in ESI$^+$ (see **Figure 8**). The signals were detected with a RT of 17.2 min. Both signals existed from day 0 until the end of the experiment. The levels of both increased until maximum around day 10. The rest of the experiment showed a slight decrease with signals yet detectable at day 105. The slight decrease could be due to simultaneous formation and disappearance.

The compound was provisionally characterized to be a dihydroxy derivative of HMPMA. Although malonamic acids are known to have small RTs (*16*), possible N-oxidation and intramolecular H-bonding can increase the RT.

Because the nonlabeled compound exhibited an odd mass, it contained an odd number of nitrogen atoms. Compared to the mass of HMPMA of 225, the mass difference was 32, corresponding to the introduction of two additional hydroxy groups, either in the aromatic part of the molecule or as an N-oxidation.

A different kind of metabolite observed in this experiment was masses 287 and 290 detected as *m/z* 288 and 291 at RT = 17.3 min in ESI$^+$ for MBOA and [D$_3$]-MBOA incubation samples, respectively (see **Figure 9**). The metabolite was present in a significant amount from day 0, increasing to its maximum around day 4. The concentration decreased rapidly from here on until around day 14, followed by a slight decrease to the end of the experiment.

The mass of the transformation product was consistent with an isomer of nitro-AMPO. The metabolite had an odd mass for
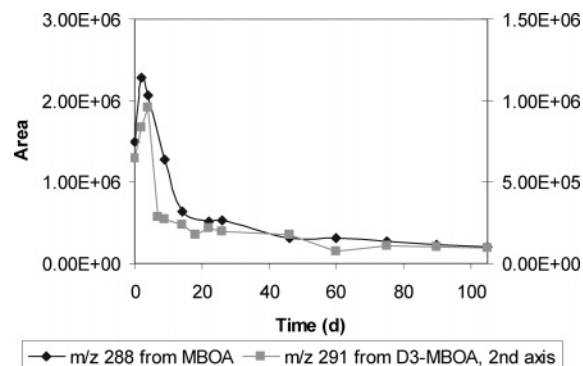
Fate and Effects of Allelochemicals

J. Agric. Food Chem., Vol. 54, No. 4, 2006   **1083**

Figure 9. Formation and disappearance of mass 287 (*m/z* 288) and 290 (*m/z* 291) from MBOA and [D₃]-MBOA, respectively, measured using ESI⁺ (RT = 17.3 min). Area is measured as a function of time with initial concentrations of MBOA and [D₃]-MBOA of 400 *μ*g/g in Flakkebjerg soil.
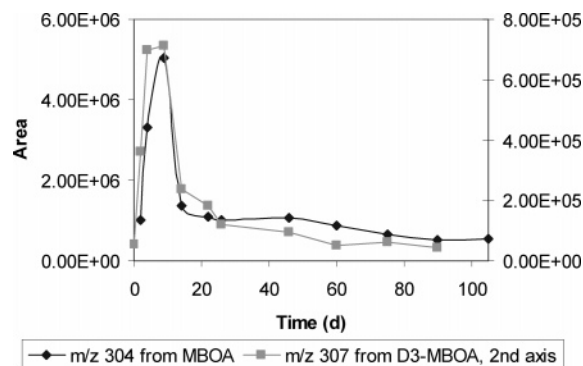

Figure 10. Formation and disappearance of mass 303 (*m/z* 304) and 306 (*m/z* 307) from MBOA and [D₃]-MBOA, respectively, measured using ESI⁺ (RT = 16.1 min). Area is measured as a function of time with initial concentrations of MBOA and [D₃]-MBOA of 400 *μ*g/g in Flakkebjerg soil.

the nonlabeled compound, implying the presence of an odd number of nitrogen atoms. When this metabolite is compared to AMPO, the difference regarding mass was 45 *m/z* values, corresponding to a nitrated derivative. The fact that acetamides could be nitrated via endophytic fungi (*16*) makes this a plausible hypothesis.

In ESI⁺ masses 303 and 306 were observed at RT = 16.1 min as *m/z* 304 and 307 for the MBOA and [D₃]-MBOA incubation samples, respectively. This is illustrated in **Figure 10**. The signal appeared at day 2, reaching maximum on day 9 and followed by a decrease until a constant minimum from day 20 throughout the time of the experiment. This was likely to be an isomer of nitro-hydroxy-AMPO according to the RT as well as the difference in mass relative to mass 287, which corresponded to an isomer of nitro-AMPO. When **Figure 4**, the formation of AMPO, is compared with **Figure 9**, the formation of nitro-AMPO, and **Figure 10**, the formation of hydroxy-nitro-AMPO, the development of the curves during time supports this theory. AMPO is formed quickly because it is present at day 0. Nitro-AMPO can thus be formed from day 0 as well, whereas hydro-nitro-AMPO seems to not be present in significant amounts until day 1. It must be stressed that the formation of a metabolite of AMPO should not be expected to coincide with the decline of the AMPO curve. During the increase of the curve, the formation of the compound is faster than the disappearance (= further transformation), but disappearance may have occurred. Mass 303 corresponded to a metabolite containing an odd number of nitrogen atoms for nonlabeled compounds. Therefore, it seemed to be reasonable to expect a nitrated derivative because this is a convenient path
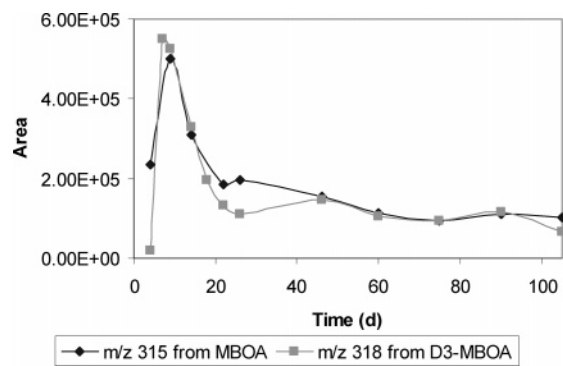

Figure 11. Formation and disappearance of mass 316 (*m/z* 315) and 319 (*m/z* 318) from MBOA and [D₃]-MBOA, respectively, measured using ESI⁻ (RT = 16.5 min). Area is measured as a function of time with initial concentrations of MBOA and [D₃]-MBOA of 400 *μ*g/g in Flakkebjerg soil.

for biotransformation (*16*). The metabolite still contained the original methyl group as established by the appearance in both kinds of incubation samples at *m/z* values differing by 3.

Masses 316 and 319 were observed in ESI⁻ as *m/z* 315 and 318 from MBOA and [D₃]-MBOA incubation samples, respectively. Consequently, the integrity of the original methyl group was conserved. Both illustrations are included in **Figure 11**, showing a maximum at day 9. The concentration decreased rapidly until day 20, followed by a slight decrease throughout the rest of the experiment. The signals were observed with RT = 16.5 min. *N*-(Acetyl)-dihydroxy-AMPO, *N*-(hydroxyacetyl)-hydroxy-AMPO, or N-oxidized isomers are the most likely candidates, reflecting the lowered RT relative to AMPO. The even mass for the nonlabeled compound corresponded to an even number of nitrogen atoms present in the molecule. The difference in mass relative to AMPO was 74 amu. The fact that OH groups lower the RT implies an AMPO oxidation product. The presence of two such groups rendered 42 amu most likely to be an acetyl group conforming to the mentioned provisionally characterized compounds. The time course of the formation of the metabolites in **Figures 5**, **9**, **10**, and **11** indicates that the addition of hydroxy and nitro groups in the AMPO molecule is a faster process than the addition of the acetyl group.

These results show a new range of transformation products not detected before. A large number of transformation products were discovered in previous experiments, emphasizing the importance of further investigation in this field. A total outline of the degradation path or transformation path of biologically active secondary metabolites from cereals is crucial if the properties of the cereals for producing these compounds are to be utilized as a viable alternative to synthetic pesticides. The target effect of these compounds toward soilborne pests and insects and toward weeds depends on the biological effects of the transformation products. The relatively limited knowledge of the environmental impact of the degradation products makes further identification needed as well.

The identities of the new transformation products described in this paper have been provisionally characterized and are under further investigation in our laboratory.

Etzerodt et al.

istry, Copenhagen University, for support and advice. We thank Kirsten Jensen for doing a competent linguistic review of the manuscript.

LITERATURE CITED

(1) Yue, Q.; Bacon, C. W.; Richardson, M. D. Biotransformation of 2-benzoxazolinone and 6-methoxy-benzoxazolinone by *Fusarium moniliforme. Phytochemistry* **1998**, *48*, 451−454.

(2) Gents, M. B.; Nielsen, S. T.; Mortensen, A. G.; Christophersen, C. Transformation products of 2-benzoxazolinone (BOA) in soil. *Chemosphere* **2005**, *61*, 74−84.

(3) Understrup, A. G.; Ravnskov, S.; Hansen, H. C. B.; Fomsgaard, I. S. Biotransformation of 2-benzoxazolinone to 2-amino-3*H*-phenoxazin-3-one and 2-acetylamino-3*H*-phenoxazin-3-one in soil. *J. Chem. Ecol.* **2005**, *31*, 1205−1222.

(4) Kumar, P.; Gagliardo, R. W.; Chilton, W. S. Soil transformation of wheat and corn metabolites MBOA and DIM₂BOA into aminophenoxazinones. *J. Chem. Ecol.* **1993**, *19*, 2453−2461.

(5) Macías, F. A.; Oliveros-Bastidas, A.; Mariän, D.; Castellano, D.; Simonet, A. M.; Molinillo, J. M. G. Degradation studies on benzoxazinoids. Soil degradation dynamics of 2,4-dihydroxy-7-methoxy-(2*H*)-1,4-benzoxazin-3(4*H*)-one (DIMBOA) and its degradation products, phytotoxic allelochemicals from Gramineae. *J. Agric. Food Chem.* **2004**, *52*, 6402−6413.

(6) Fomsgaard, I. S.; Mortensen, A. G.; Gents, M. B.; Understrup, A. G. Time-dependent transformation of varying concentrations of the hydroxamic acid metabolites MBOA and BOA in soil. *Proceedings, Second European Allelopathy Symposium. Allelopathy−from Understanding to Application, FATEALLCHEM Workshop ("Fate and Toxicity of Allelochemicals (Natural Plant Toxins) in Relation to Environment and Consumer")*, June 3−5; Institute of Soil Science and Plant Cultivation Press Services: Pulawy, Poland; 2004; pp 61−63.

(7) Barry, C. E.; Nayar, P. G.; Begley, T. P. Phenoxazinone synthase: enzymatic catalysis of an aminophenol oxidative cascade. *J. Am. Chem. Soc.* **1988**, *110*, 3333−3334.

(8) Barry, C. E.; Nayar, P. G.; Begley, T. P. Phenoxazinone synthase: mechanism for the formation of the phenoxazinone chromophore of actinomycin. *Biochemistry* **1989**, *28*, 6323−6333.

(9) Eggert, C.; Temp, U.; Dean, J. F. D.; Eriksson, K. L. Laccase-mediated formation of the phenoxazinone derivative, cinnabarinic acid. *FEBS Lett.* **1995**, *376K*, 202−206.

(10) Maruyama, K.; Moriguchi, T.; Mashino, T.; Nishinaga, A. Highly selective formation of 2-amino-phenoxazin-3-one by catalytic oxygenation of *o*-aminophenol. *Chem. Lett.* **1996**, *9*, 819−820.

(11) Simandi, L. I.; Barna, T.; Nemeth, S. Kinetics and mechanism of the cobaloxime(II)-catalyzed oxidation of 2-aminophenol by dioxygen. A phenoxazinone synthase model involving free-radical intermediates. *J. Chem. Soc.* **1996**, *4*, 473−478.

(12) Simandi, L. I.; Besenyei, G. Kinetics and mechanisms of the transition metal complexes. *Acta Pharm. Hung.* **2000**, *70*, 244−250.

(13) Kim, K.; Cho, S. Purification and characterization of phenoxazinone synthase from *Streptomyces* sp. V-8 mutant producing adenosine deaminase inhibitor. *Yakhak Hoechi* **1999**, *43*, 68−76.

(14) Gagliardo, R. W.; Chilton, W. S. Soil transformation of 2-(3*H*)-benzoxazolinone of rye into phytotoxic 2-amino-(3*H*)-phenoxazin-3-one. *J. Chem. Ecol.* **1992**, *18*, 2453−2461.

(15) Friebe, A.; Villich, V.; Hennig, L.; Kluge, M.; Sicker, D. Tolerance of *Avena sativa* to the allelochemical benzoxazolinone. Degradation of BOA by root-colonizing bacteria. *J. Appl. Bot.* **1998**, *64*, 2386−2391.

(16) Zikmundova, M.; Drandarov, K.; Bigler, L.; Hesse, M.; Werner, C. Biotransformation of 2-benzoxazolinone and 2-hydroxy-1,4-benzoxazin-3-one by endophytic fungi isolated from *Aphelandra tetragona. Appl. Environ. Microbiol.* **2002**, *68*, 4863−4870.

(17) Macías, F. A.; Marín, D.; Oliveros-Bastidas, A.; Chinchilla, D.; Simonet, A. M.; Molinillo, J. M. G. Isolation and synthesis of allelochemicals from Gramineae: benzoxazinones and related compounds. *J. Agric. Food Chem.* **2006**, *54*, 991−1000.

(18) Quast, H.; Bieber, L. Synthese und Photolyse von 1,4-Dialkyl-1,4-dihydro-5*H*-tetrazol-5-onen und -thionen: Neue Wege zu Diaziridinonen und Carbodiimiden. *Chem. Ber.* **1981**, *114*, 3253−3272.

(19) Bird, C. W.; Brown, A. L.; Chan, C. C. A new type of abnormal Reimer−Tiemann reaction. *Tetrahedron* **1985**, *41*, 4688−4689.

(20) Perkin, W. H., Jr.; Rây, J. N.; Robinson. Experiments on the synthesis of brazilin and hæmatoxylin and their derivatives. *R., J. Chem. Soc.* **1926**, 945.

(21) Maleski, R. J. Improved procedures for the preparation of 2-nitro-5-methoxyphenol and 6-methoxy-2(3*H*)-benzoxazolone from 3-methoxyphenol. *Synth. Commun.* **1993**, *23*, 343−348.

(22) Greve, M. H.; Helweg, A.; Yli-Halla, M.; Eklo, O. M.; Nyborg, Å. A.; Solbakken, E.; Öborn, I.; Stenström, J. Nordic Reference Soils Annex 1. In *Nordic Reference Soils: 1. Characterization and Classification of 13 Typical Nordic Soils 2. Sorption of 2,4-D, Atrazine and Glyphosate*; Tiberg, E., Ed.; TemaNord Environment, Nordic Council of Ministers: Copenhagen, Denmark, 1998; Vol. 537, pp 70−72.

(23) Fomsgaard, I. S.; Mortensen, A. G.; Idinger, J.; Coja, T.; Bluemel, S. Transformation of benzoxazinones and derivatives and microbial activity in the test environment of soil ecotoxicological tests on *Poecilus cupreus* and *Folsomia candida. J. Agric. Food Chem.* **2006**, *54*, 1086−1092.

(24) Andersen, O. A.; Flatmark, T.; Hough, E. Crystal structure of the ternary complex of the catalytic domain of human phenylalanine hydroxylase with tetrahydrobiopterin and 3-(2-thienyl)-L-alanine and its implications for the mechanism of catalysis and substrate activation. *J. Mol. Biol.* **2002**, *320*, 1095−1108.

(25) Erlandsen, H.; Kim, J. Y.; Patch, M. G.; Han, A.; Volner, A.; Abu-Omar, M. M.; Stevens, R. C. Structural comparison of bacterial and human iron-dependent phenylalanine hydroxylases: similar fold, different stability and reaction rates. *J. Mol. Biol.* **2002**, *320*, 645−661.

(26) Kinzie, S. D.; Thevis, M.; Ngo, K.; Whitelegge, J.; Loo, J. A.; Abu-Omar, M. M. Posttranslational hydroxylation of human phenylalanine hydroxylase is a novel example of enzyme self-repair within the second coordination sphere of catalytic iron. *J. Am. Chem. Soc.* **2003**, *125*, 4710−4711.

(27) Maass, A.; Scholz, J.; Moser, A. Modeled ligand-protein complexes elucidate the origin of substrate specificity and provide insight into catalytic mechanisms of phenylalanine hydroxylases and tyrosine hydroxylases. *Eur. J. Biochem.* **2003**, *270*, 1065−1075.

(28) Wang, L.; Erlandsen, H.; Haavik, J.; Knappskog, P. M.; Stevens, R. C. Three-dimensional structure of human tryptophan hydroxylase and its implications for the biosynthesis of the neurotransmitters serotonin and melatonin. *Biochemistry* **2002**, *41*, 12569−12574.

(29) Xu, D.; Enroth, C.; Lindqvist, Y, Ballou, D. P.; Massey, V. Studies of the mechanism of phenol hydroxylase: effect of mutation of praline 364 to serine. *Biochemistry* **2002**, *41*, 13627−13636.

(30) Zheng, Y.; Dong, J.; Palfey, B. A.; Carey, P. R. Using Raman spectroscopy to monitor the solvent-exposed and "buried" forms of flavin in *p*-hydroxybenzoate hydroxylases. *Biochemistry* **1999**, *38*, 16727−16732.

(31) Munro, A. W.; Leys, D. G.; McLean, K. J.; Marshall, K. R.; Ost, T. W. B.; Daff, S.; Miles, C. S.; Chapman, S. K.; Lysek, D. A.; Moser, C. C.; Dutton, P. L. P450 μ_B3: the very model of a modern flavocytochrome. *Trends Biochem. Sci.* **1992**, *27*, 250.

(32) Chang, A.; Hartmann, T. Solubilization and characterization of a senecionine *N*-oxygenase from *Crotalaria scassellatii* seedlings. *Phytochemistry* **1998**, *49*, 1859−1866.

(33) Koch, B. M.; Sibbesen, O.; Halkier, B. A.; Svendsen, I.; Møller, B. L. The primary sequence of cytochrome P450tyr, the multifunctional *n*-hydroxylase catalyzing the conversion of L-tyrosine to *p*-hydroxyphenylacetaldehyde oxime in the biosynthesis of the cyanogenic glucoside Dhurrin in *Sorghum bicolour* (L.) Moench. *Arch. Biochem. Biophys.* **1995**, *323*, 177−186.

(34) Leighton, V.; Niemeyer, H. M.; Jonsson, L. M. V. Substrate specificity of a glucosyltransferase and an *N*-hydroxylase involved in the biosynthesis of cyclic hydroxamic acids in Gramineae. *Phytochemistry* **1994**, *36*, 887−892.

(35) Naumann, C.; Hartmann, T.; Ober, D. Evolutionary recruitment of a flavin-dependent monooxygenase for the detoxification of host plant-acquired pyrrolizidine alkaloids in the alkaloid-defended arctiid moth *Tyria jacobaeae*. *Proc. Natl. Acad. Sci. U.S.A.* **2002**, *99*, 6085−6090.

(36) Wittstock, U.; Halkier, B. A. Cytochrome P450 CYP79A2 from *Arabidopsis thaliana* L. catalyzes the conversion of L-phenylalanine to phenylacetaldoxime in the biosynthesis of benzylglucosinolate. *J. Biol. Chem.* **2000**, *275*, 14659−14666.

(37) Christensen, A. B.; Gregersen, P. L.; Olsen, C. E.; Collinge, D. B. A flavonoid-7-*O*-methyltransferase is expressed in barley leaves in response to pathogen attack. *Plant Mol. Biol.* **1998**, *36*, 219−227.

(38) Fomsgaard, I. S.; Mortensen, A. G.; Carlsen, S. C. K. Microbial transformation products of benzoxazolinone and benzoxazinone allelochemicals—a review. *Chemosphere* **2004**, *54*, 1025−1038.

(39) Zikmundova, M.; Drandarov, K.; Hesse, M.; Werner, C. Hydroxylated 2-amino-3*H*-phenoxazin-3-one derivatives as products of 2-hydroxy-1,4-benzoxazin-3-one (HBOA). Biotransformation by *Chaetosphaeria* sp. an endophytic fungus from *Aphelandra tetragona*. *Z. Naturforsch.* **2002**, *57C*, 660−665.

(40) Friebe, A.; Wieland, I.; Schulz, M. Tolerance of *Avena sativa* to the allelochemical benzoxazolinone. Degradation of BOA by root-colonizing bacteria. *J. Appl. Bot.* **1996**, *70*, 150−154.

(41) Sicker, D.; Frey, M.; Schulz, M.; Geirl, A. Role of natural benzoxazinones in the survival strategy of plants. *Int. Rev. Cytol.* **2000**, *198*, 319−346.

(42) Alberts, B.; Bray, D.; Lewis, J.; Raff, M.; Roberts, K.; Watson, J. D. Chemical signaling between cells. In *Molecular Biology of the Cell*; Garland Publishing: New York, 1983; pp 760−763.